Expanded View Figures

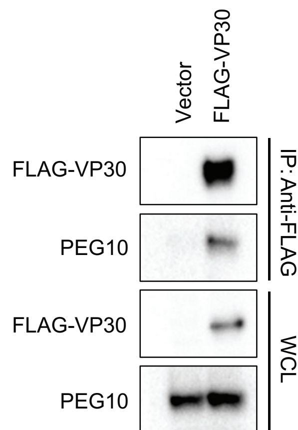

Figure EV1. Co-immunoprecipitation between VP30 and endogenous PEG10.

Huh7 cells were transfected with empty vector (Vector) or FLAG-VP30 expression plasmid. IPs (IP: Anti-FLAG) and whole-cell lysates (WCL) were analyzed by Western blotting with anti-FLAG or anti-PEG10 antibodies.

Figure EV2. VP30 does not bind to the native VP40 proline-tyrosine motif but does bind to bat RBBP6.

A Co-immunoprecipitation assay to assess HA–VP40 interaction with FLAG-VP30. HEK293T cells were transfected with HA-VP40 plasmid and either empty vector or FLAG-VP30 plasmid. An anti-FLAG immunoprecipitation (IP) was performed. IP and WCL were analyzed by Western blotting with anti-HA and anti-FLAG antibodies. An anti-β-tubulin Western blot provided a loading control.

B Anti-GFP immunoprecipitation of HA-VP30 with GFP fusions to wild-type or mutated VP40-derived peptides (GFP-VP40, GFP-VP40_mut1, or GFP-VP40_mut2). GFP without a fusion partner (GFP) and GFP fused to RBBP6 peptide (GFP-RBBP6) served as controls. Immunoblots with anti-HA, anti-GFP, and anti-β-tubulin are shown.

C GFP fused to peptides derived from human and bat (*Rousettus aegyptiacus*) RBBP6 were expressed along with HA-VP30. Co-immunoprecipitation was performed using anti-GFP magnetic beads, and representative immunoblots for IP and WCL are shown.

D Equilibrium dissociation curves of FITC-RBBP6 peptide to $eVP30_{130\text{-}272}$ as it is outcompeted by increasing concentrations (0.13–500 μM) of human and bat RBBP6 peptides. Fluorescence polarization was determined with constant concentrations of FITC-RBBP6 and $eVP30_{130\text{-}272}$, at 0.50 μM and 3.8 μM, respectively. Experiments were performed in two independent replicates. Error bars represent standard deviation.

E MG activity upon titration of GFP fused to human and bat-derived RBBP6 peptides (12.5 ng and 125 ng). GFP alone was used as a control. Reporter activity was read at 48 h post-transfection and fold MG activity was calculated relative to a no VP30 control. # denotes statistical significance compared with RBBP6 peptide for each dose. The data represent the mean ± SD from one representative experiment in which each transfection condition was performed in triplicate ($n = 3$). Each experiment was reproduced in at least two additional, independent experiments (see Appendix Fig S1). Statistical significance was calculated relative to GFP control for each concentration tested using ANOVA with Tukey's multiple comparisons test. $^{****}P < 0.00005$; $^{\#\#}P < 0.005$, $^{*}P < 0.05$

© 2021 The Authors

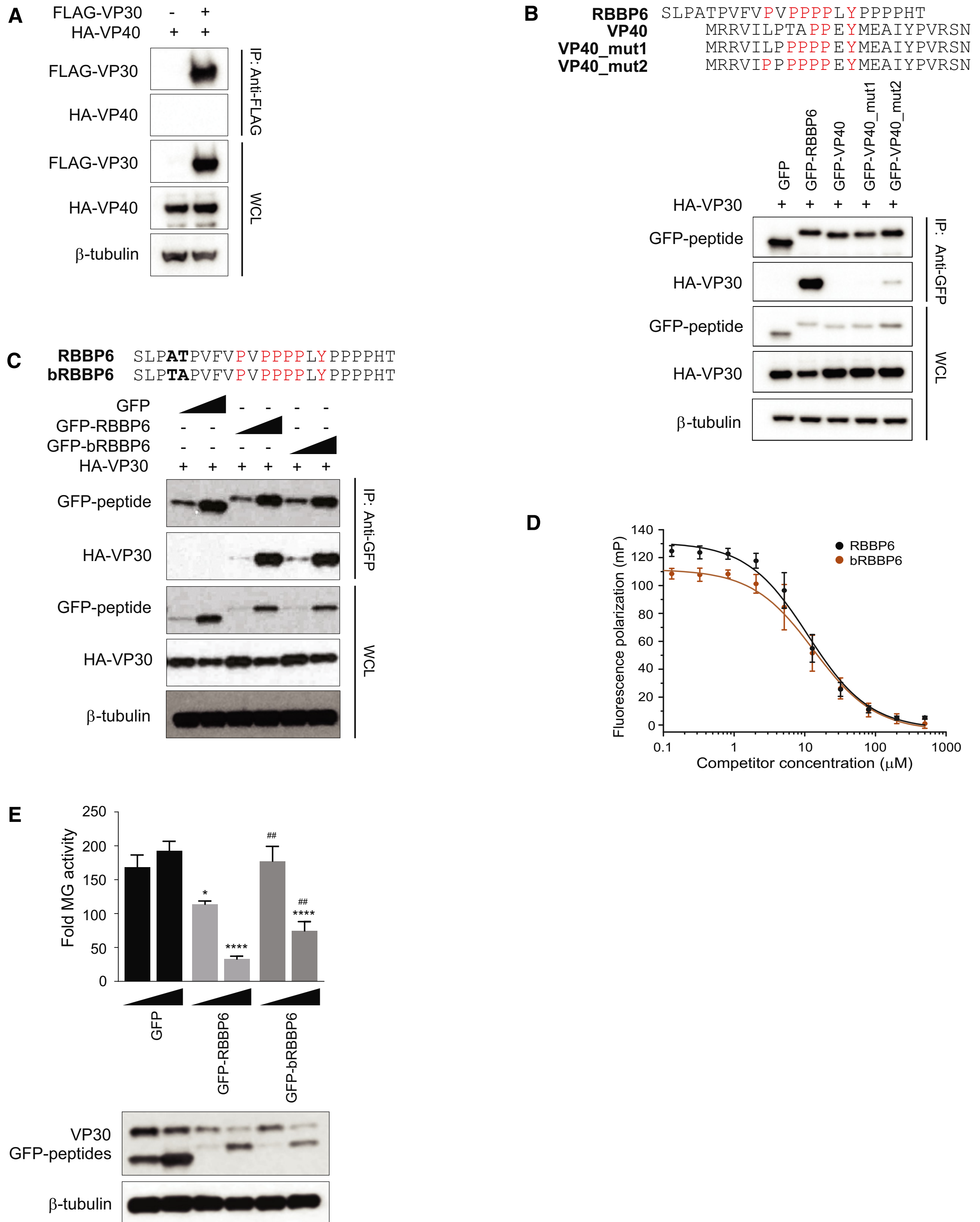

Figure EV2.

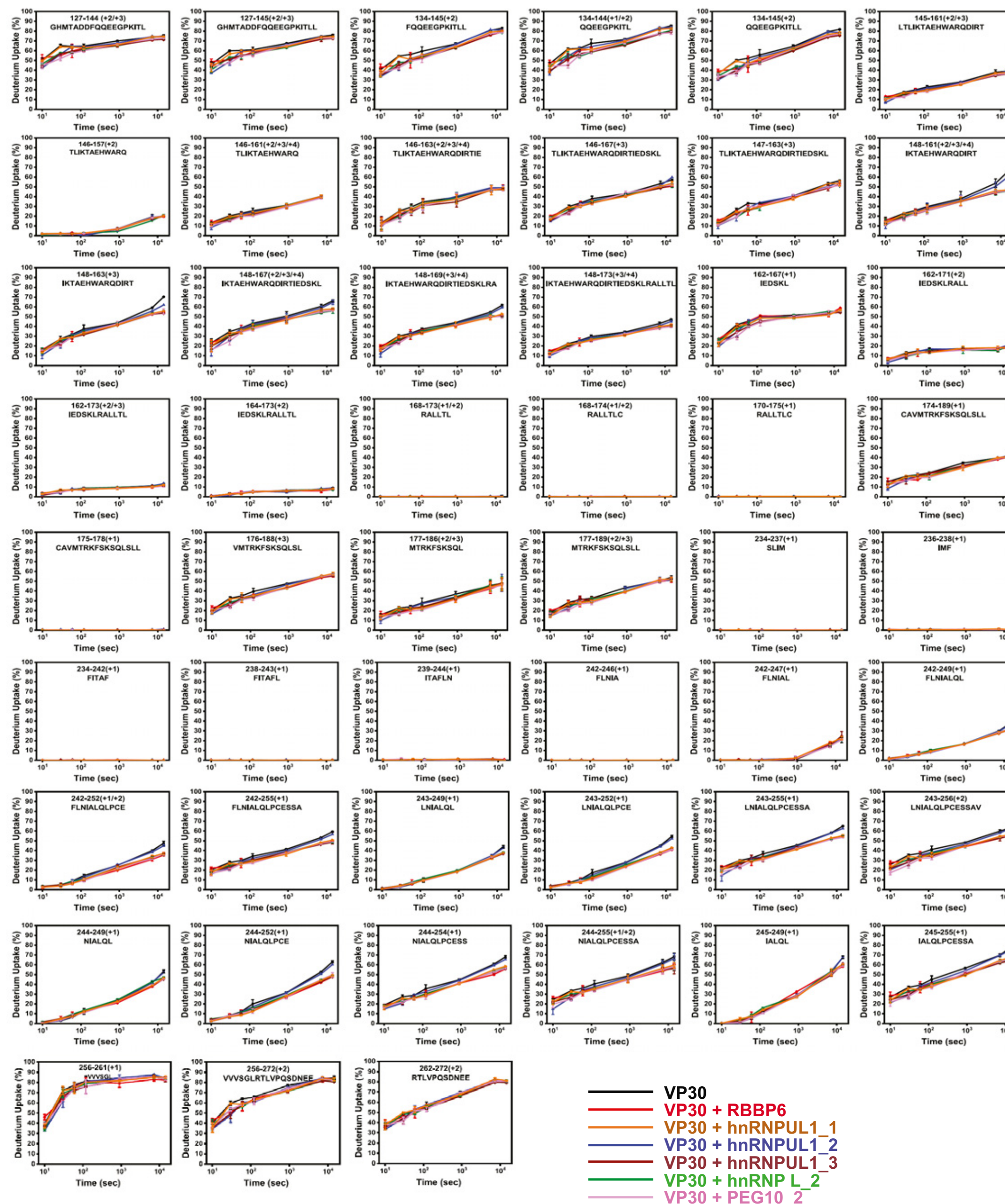

Figure EV3. HDX kinetic plots for all VP30 peptides.

 © 2021 The Authors

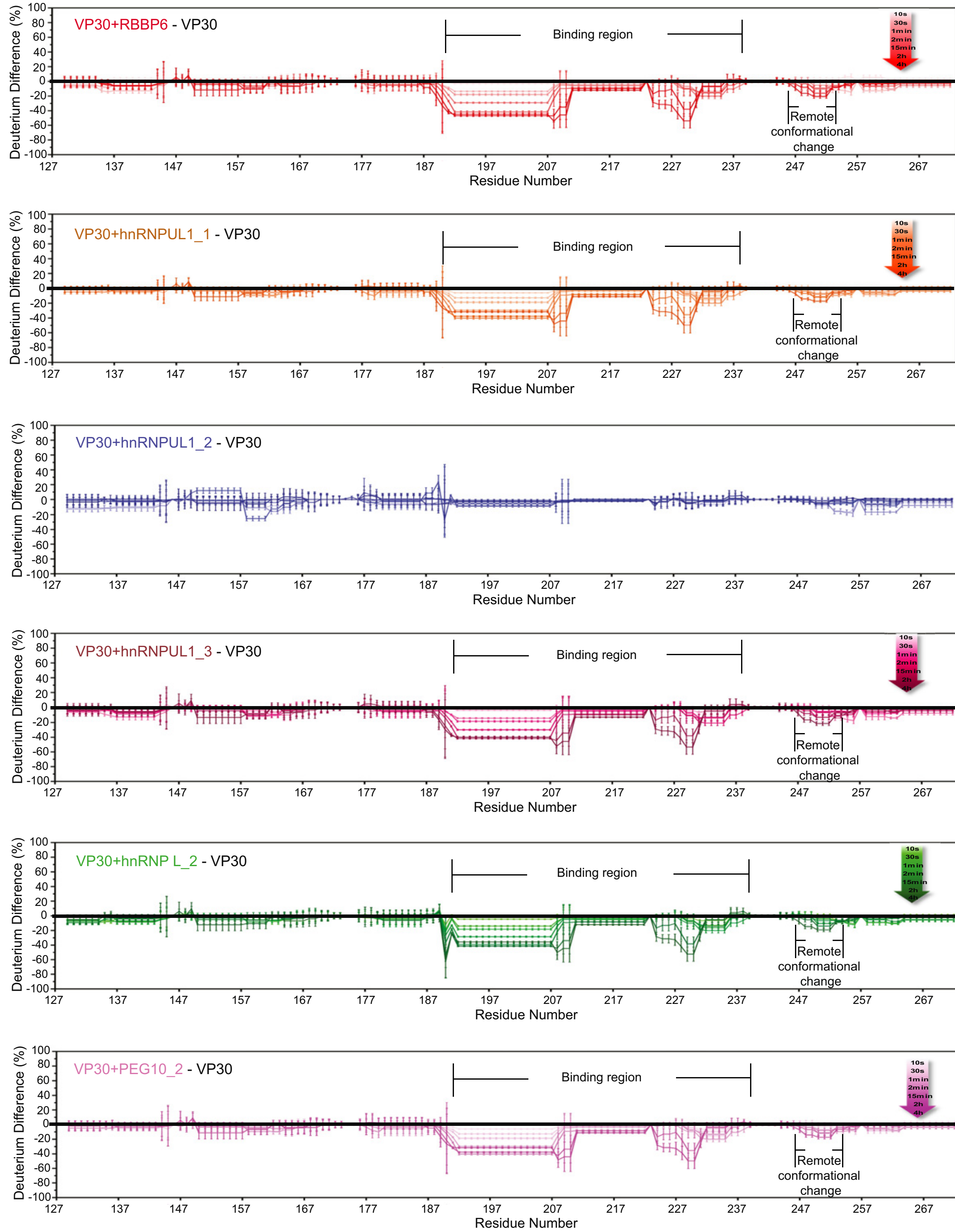

Figure EV4. Statistical analysis of deuterium uptake differences of all time points confirms the binding regions.

Deuterium uptake differences between different bound VP30 and unbound VP30 were calculated for each time point from 10 s to 4 h, and are depicted by gradient colors. Standard deviation between triplicates was calculated separately for each time point representing the bound and unbound states. Plotted on the graph is a threefold propagation error of each time point as shown by the error bars, giving 99.7% certainty on the observed difference. VP30 bound with RBBP6, hnRNPUL1_1, hnRNPUL1_3, hnRNP L_2, and PEG10_2 showed the same binding regions and similar regions exhibiting remote conformational or dynamics reduction owing to binding. There is no significant difference for VP30 with hnRNPUL1_2; therefore, it served as a negative control.

© 2021 The Authors

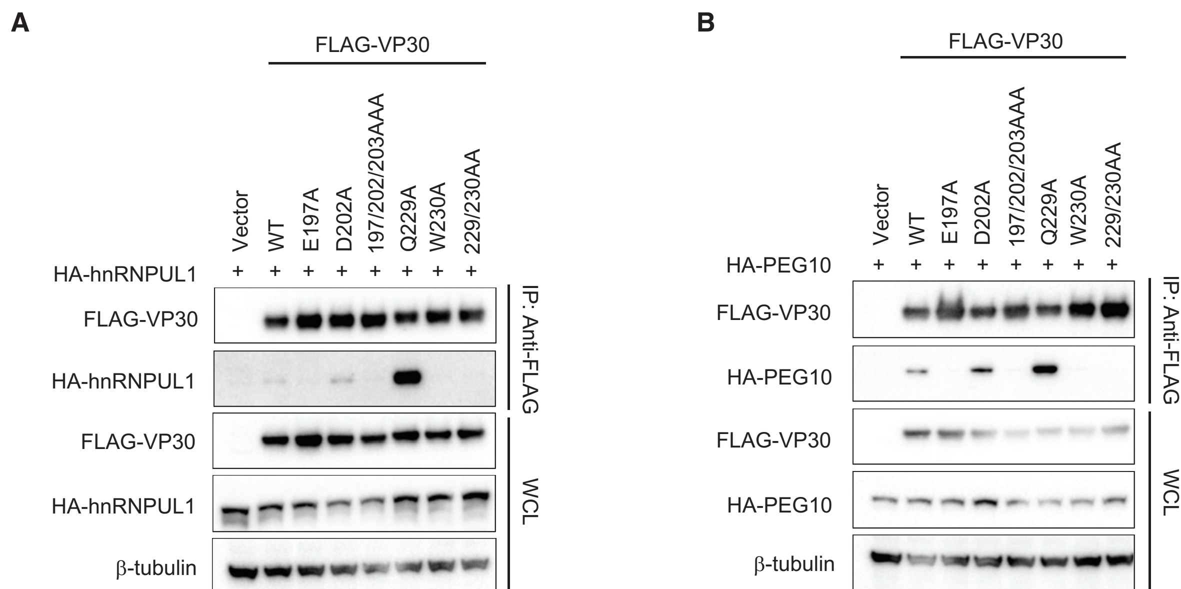

Figure EV5. Interaction of VP30 point mutants with hnRNPUL1 and PEG10.

A, B Representative Western blots of co-immunoprecipitation experiments to assess interaction between the indicated VP30 mutants and hnRNPUL1 (A) or PEG10 (B).

Figure EV6. Effects of host PPxPxY proteins on replication-defective and VP30-independent minigenome assays.

A MG activity upon over-expression of each of the indicated host proteins using WT or replication-deficient MG systems. 293T cells were transfected with plasmids encoding FLAG-tagged host proteins along with the MG plasmids. Fold MG activity was calculated relative to a no VP30 control.

B MG activity upon over-expression of each of the host protein using the 5′ UTR mutant MG as a template.

C MG activity upon over-expression of GFP or hnRNPUL1 peptide 3 fused to GFP in combination with full-length (FL) hnRNPUL1 (doses 12.5 ng and 125 ng). Statistical significance was calculated relative to the GFP control for each concentration tested using ANOVA with Tukey's multiple comparisons test.

Data information: For each panel (A–C), the data represent the mean ± SD from one representative experiment in which each transfection condition was performed in triplicate ($n = 3$). Each experiment was reproduced in an additional, independent experiment (see Appendix Figs S5–S7). ****$P < 0.00005$; ***$P < 0.0005$, **$P < 0.005$.

▶

 © 2021 The Authors

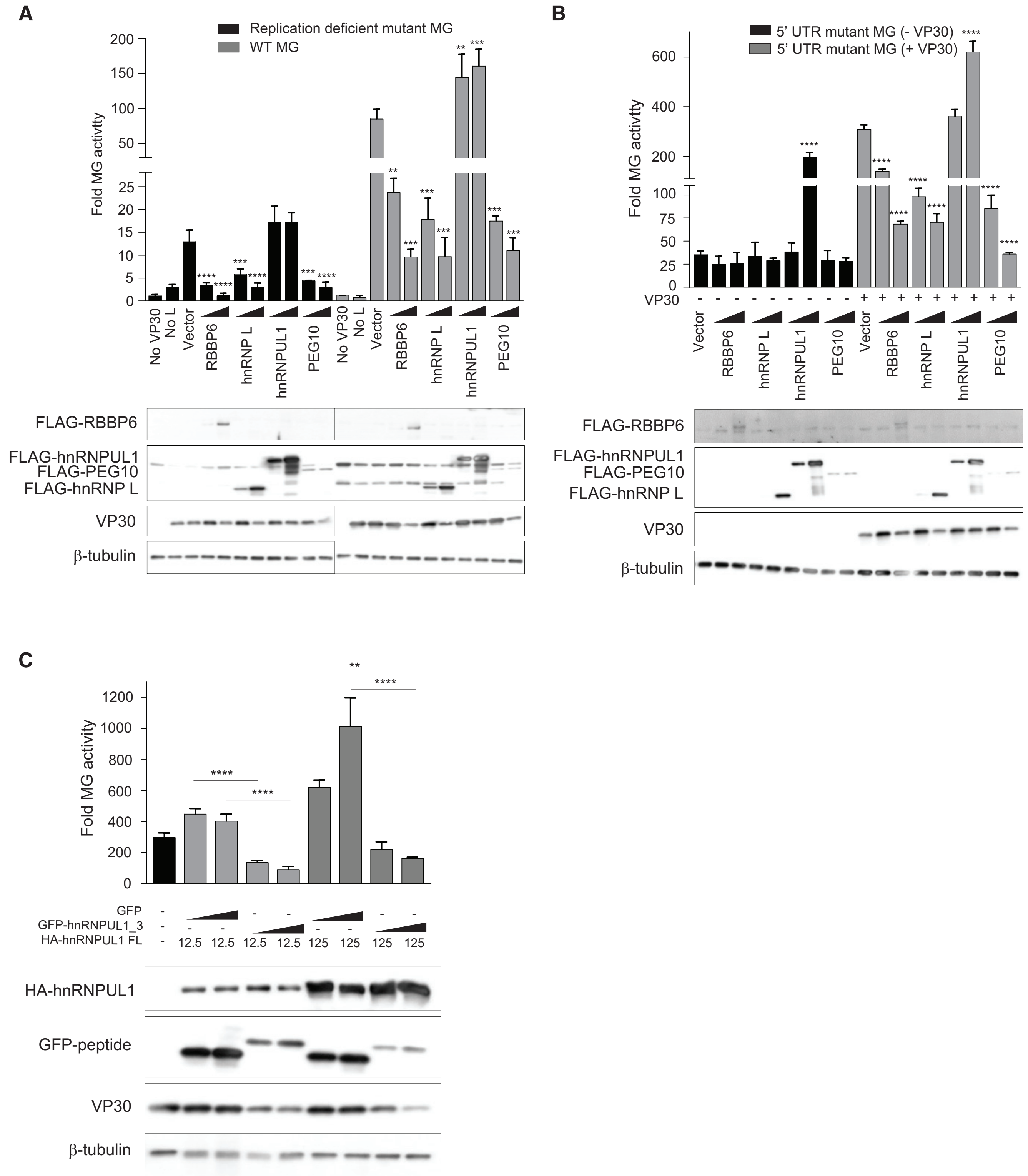

Figure EV6.